The Seventh Asian-Pacific Symposium on Structural Reliability and Its Applications (APSSRA2020)
October 4–7 2020, Tokyo, Japan
T. Takada, I. Yoshida & T. Itoi (editors)

Validation of Variation in Synthetic Ground Motions Caused by Variability of Seismic-Source Characteristics

M. Aoki[1], S. Igarashi[2], Y. Uchiyama[3], S. Sakamoto[4]

[1]*Taisei Corporation. Email: aokmss00@pub.taisei.co.jp*
[2] *Taisei Corporation. Email: igrsyk00@pub.taisei.co.jp*
[3]*Taisei Corporation. Email: yasuo.uchiyama@sakura.taisei.co.jp*
[4]*Taisei Corporation. Email: shigehiro.sakamoto@sakura.taisei.co.jp*

Abstract: Recent years, a method to generate synthetic ground motions using finite fault models has been employed in the process of probabilistic seismic hazard analysis (PSHA). This method is based on Monte Carlo simulation (MCS), which incorporate the uncertainties of seismic-source characteristics. For conducting more precise PSHA, however, it is important to validate whether the simulated ground motions with uncertainty could cover realistic ground motion level at specific site. In this paper, the authors validated simulated ground motions based on stochastic fault models by comparing them with observed strong motion records at KiK-net stations by NIED during the 2016 Kumamoto earthquake foreshock (M_{JMA} 6.5) April 14 as an example.
The stochastic Green's function method (SGFM), which takes uncertainties of seismic-source parameters into account, is employed for ground motion calculation. In general, the seismic-source uncertainties can be classified into epistemic uncertainties due to different empirical equations for macro-scopic which are considered by logic-tree, and into aleatory uncertainties due to randomness of micro-scopic characteristics which are considered by MCS. For simple comparison with synthetic and observed ground motions during the foreshock, only aleatory uncertainties are considered. The macro-scopic characteristics, such as a magnitude and location of the fault, are fixed to estimated values for the foreshock, in this paper.
As a result, it was indicated that the simulated ground motions could cover observed ground motion level in short-period range. The multiple linear regression analysis yielded that stress-drop parameter, fmax, and location of 1st asperity had high sensitivity to pseudo velocity response of the MCS results. In this study, however, only short-period range was targeted because SGFM could not reproduce the foreshock in long-period range. In a study by Igarashi et al. (2015), the hybrid method of SGFM and wave-number integration method were conducted to generate synthetic ground motions. It is necessary that we apply the hybrid method to generate synthetic ground motions.

Keywords: fault model, variation in seismic ground motions, aleatory uncertainty, the Kumamoto Earthquake.

1. Introduction

In recent years, synthetic ground-motions simulated based on finite fault models have been utilized for probabilistic seismic hazard analysis (PSHA) of nuclear power plants. Nishida et al. (2015) proposed a methodology to generate a lot of ground-motion time histories which incorporate seismic-source uncertainties by Monte Carlo simulation (MCS). These ground motions are generated based on physics-based fault models that have stochastic seismic source characteristics. This method has the advantages that the seismic intensity of ground motions such as peak acceleration as well as their duration and frequency content can be considered. Therefore, these ground motions can bring about more detailed and useful information when we conduct seismic response analysis of nuclear power structures, systems, and components (SSCs), and they can contribute to appropriate decision making for seismic safety measures.

For conducting more precise PRA, however, it is important to validate whether the simulated ground motions could cover the realistic ground-motion level at specific site. In this study, synthetic ground motions using finite fault models which have stochastic seismic-source characteristics are generated, and validate them by comparing with observed strong motion records during the 2016 Kumamoto earthquake (M_{JMA}6.5, foreshock) April 14th. The Kumamoto EQ is regarded as specified fault activity, Futagawa-Hinagu fault zone. The Head- quarters for Earthquake Research Promotion (HERP) in Japan, had reported seismic source characteristics for Futagawa-Hinagu fault zone activity. The synthetic ground motions at several KiK-net stations are evaluated using 1,000 fault models with the seismic-source parameters which are median reported by HERP and the variance used in previous studies, where the magnitude and fault rupture area are fixed. The influence of the uncertainties of seismic-source characteristics on the synthetic ground motions and the validity of simulated ground motions are examined.

2. Method for ground motion calculation

The stochastic Green's function method (SGFM), which taking uncertainties of seismic-source parameters into account, is employed for ground motion calculation. The seismic-source uncertainties can be classified into epistemic uncertainties due to different empirical equations for macro-scopic (outer fault parameters) which are considered by logic-tree (LT), and into aleatory uncertainties due to randomness of micro-scopic (inner fault parameters) characteristics which are considered by MCS (Alfredo and Wilson 2006). For simple comparison with synthetic and observed ground motions during the foreshock, only aleatory uncertainties are considered, and macro-scopic characteristics, such as a magnitude, size of the fault, and location of the fault, are fixed to estimated values for the foreshock, in this paper.

2.1 Stochastic Green's function method

One thousand waves of synthetic ground motions at each KiK-net station using SGFM are generated based on Eq. 1 through 8.

$$A(f) = \frac{R_{\theta\phi} \cdot FS \cdot P_{RTITN}}{4\pi\rho\beta^3} \cdot M_0 \cdot \frac{(2\pi f)^2}{1+(f/f_c)^2} \cdot \frac{1}{\sqrt{1+(f/f_{max})^m}} \cdot \frac{1}{R_c} \cdot exp\left[-\frac{\pi f R}{Q(f)\beta}\right] \quad (1)$$

$$f_c = 4.9 \times 10^6 \beta (\Delta\sigma/M_0)^{1/3} \quad (2)$$

$$Q(f) = Q_0 f^{\alpha} \quad (3)$$

$$\tau = \alpha_{tr} \cdot \frac{W}{V_r} \quad (4)$$

$$C_{Sa} = \frac{S_a}{S} \quad (5)$$

$$C_{Sa12} = \frac{S_{a1}}{S_{a2}} \quad (6)$$

$$C_{Da} = \frac{D_a}{D} \quad (7)$$

$$V_r = C_{V_r} \cdot \beta \quad (8)$$

where, $A(f)$ is the Fourier amplitude spectrum if ground motion acceleration from discrete fault element, $R_{\theta\phi}$ is the radiation pattern coefficients, FS is the amplification due to the free surface, P_{RTITN} is the reduction factor that accounts for the partitioning of energy into two horizontal components, and m is the coefficient of the decay rate at high frequencies. ρ is the density, M_0 is the seismic moment of the fault element, f_c is the corner frequency, β is shear velocity, $Q(f)$ is the Q-value, τ is rise time, which is the rapture time of fault element, W is the fault width, V_r is the rupture velocity, S_a is the sum of asperities area, S_{a1} is the area of 1st asperity (larger), S_{a2} is the area of 2nd asperity (smaller), S is the area of fault, D_a is the dislocation of asperity, and D is the dislocation of fault.

2.2 Uncertainties of seismic-source characteristics

In MCS, the ground motions are repeatedly generated for each fault model where realized values for stochastic parameters are given in the way that the realized values are randomly set according to the corresponding distribution of seismic-source stochastic parameter. Table 1 shows stochastic parameters in seismic-source characteristics. The medians and averages are set based on the "Recipe" for strong ground motion prediction with specified source faults by HERP, and their variance are set based on the previous study (Nishida et al. 2015).

Table 1. Stochastic parameters for seismic source characteristics.

stochastic parameters for seismic source characteristics	name	unit	distribution	λ or μ	ζ or σ
stress drop	$\Delta\sigma$	MPa	lognormal	3.00	0.50
shear wave ratio to rupture velocity	C_{Vr}	-	lognormal	0.72	0.08
rise time of coefficient	α_{tr}	-	lognormal	0.50	0.20
asperity area ratio to fault area	C_{Sa}	-	normal	0.22	0.04
the number of asperities	N_{asp}	-	1 or 2 (when C_{Sa12} is less than 0.1, N_{asp} is 1)		
ratio of small asperity area to large one	C_{Sa12}	-	normal	0.50	0.30
asperity slip dislocation ratio	C_{Da}	-	normal	2.00	0.68
rupture starting points	*startX*	-	uniform	on the bottom of the asperity	
location of the asperity	*aspX1, aspY1* *aspX2, aspY2*	- -	uniform	in the fault plane	
frequency for high-cut filter	f_{max}	Hz	lognormal	6.00	0.22

where, λ ; median, μ ; average, ζ ; log-standard deviation, σ ; standard deviation

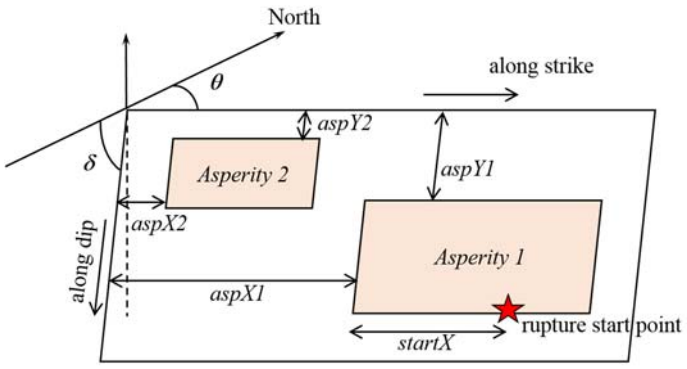

Figure 1. Notations of the fault model.

3. Reproducing the Kumamoto EQ foreshock

Kinematic source inversion results by Asano and Iwata (2016) to several macro-scopic source parameters and spectral inversion results by Uchiyama and Yamamoto (2016) to short-period spectral level A and Q-value are applied. The sum of asperity area S_a and $\Delta\sigma_a$ are calculated from M_0 and A based on Eq. 9 and 10.

$$r = \sqrt{S_a/\pi} = (7\pi/4)\left\{M_0/\left(A\cdot\sqrt{S/\pi}\right)\right\}\cdot\beta^2 \qquad (9)$$

$$A = 4\pi\cdot r\cdot\Delta\sigma_a\cdot\beta^2 \qquad (10)$$

As for micro-scopic source characteristics such as M_{0a}, location of asperities, etc., the report by Port and Airport Research Institute (PARI) are referred. They have estimated characterized fault model for the foreshock, and well reproduced the observed records by the empirical Green's function method. The location of asperities and rupture start point is shown in Fig. 3. A sub-fault size was set to 1km×1km. In order to confirm whether these parameters are included in range of the variance in Table 1, the deviations of parameters were calculated (Table 2). Although C_{Vr}, α_{tr}, and C_{Sa} seems to be somewhat far from the average (the deviations show 2~3σ), these may be possibly realized. The other parameters can be regarded as standard values.

The results of reproducing the foreshock by SGFM is shown in Fig. 4. Although synthetic ground motions are well reproduced in a short period range, long period spectral level (T >1.0s) is underestimated. Commonly, SGFM is used for simulation in short-period range, and a theoretical or numerical method is used for in long-period range. For this reason, response spectra in short-period range (T ≦1.0s) are discussed.

Table 2. Deviation of seismic-source parameters of the foreshock for SGFM

Name	Value	Deviation ζ or (σ)
$\Delta\sigma$	2.024 [MPa]	-0.787
C_{Vr}	0.60	-2.279
α_{tr}	0.28	-2.899
C_{Sa}	0.099	(-3.027)
C_{Sa12}	1.000	(1.667)
C_{Da}	1.387	(-0.901)
aspX1	0.455	(-0.156)
aspY1	0.100	(-1.387)
aspX2	0.636	(0.472)
aspY2	0.600	(0.346)
startX	0.500	(0.000)
f_{max}	6.00 [Hz]	(0.000)

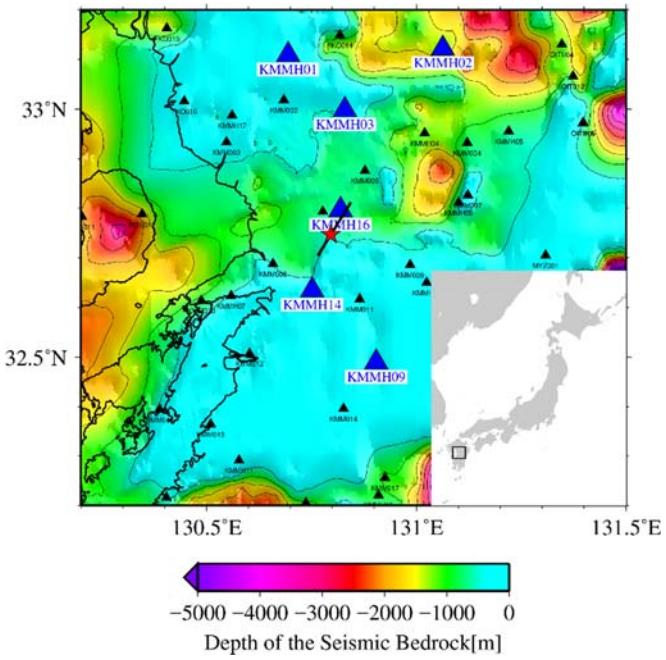

Figure 2. Location of fault of the 2016 Kumamoto earthquake foreshock and target stations. Blue triangles show target stations, and a red star shows the hypocenter of the foreshock

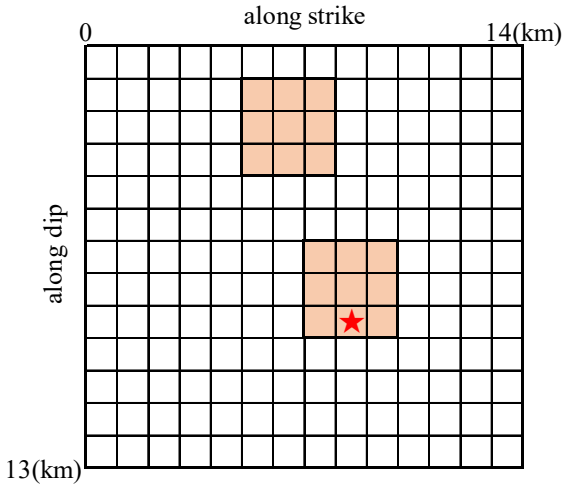

Figure 3. Location of asperities and rupture start point for reproducing the 2016 Kumamoto EQ foreshock by SGFM

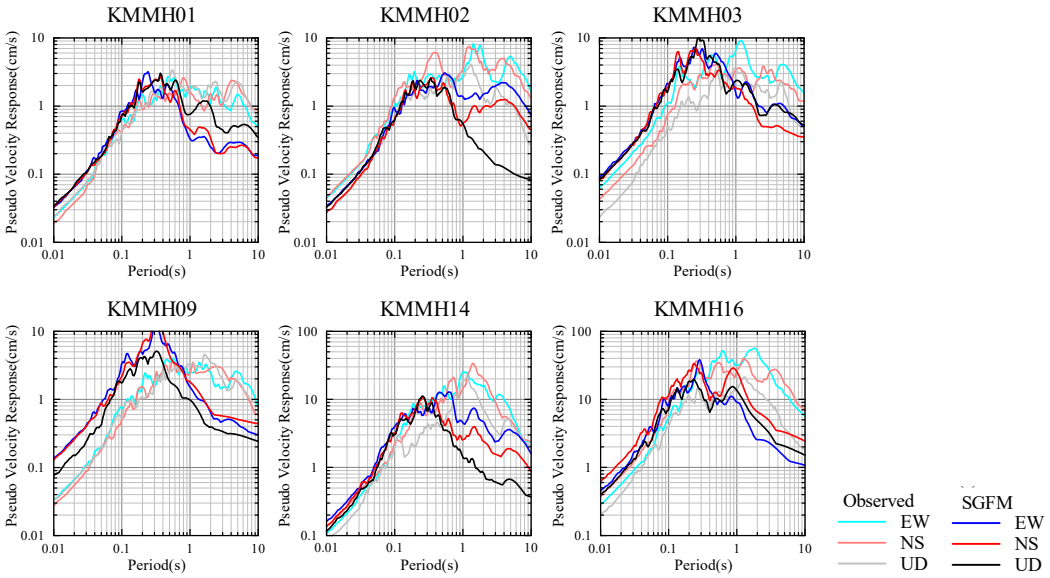

Figure 4. Comparison of response spectra (pSv, h=5%) of the Kumamoto foreshock between observed and synthetic ground motions

4. Results of Monte Carlo simulation

At each station, synthetic ground motions from 1,000 realized fault models following the distribution in Table 1 are simulated. Fig. 5 shows the response spectra obtained at KMMH01 as an example.

The deviation of pseudo velocity response of observed ground motion in lognormal space were calculated comparing with the synthetic ground motions. Fig. 6 shows the deviations of the observed response spectra for each station. It is clarified that the observed ground motions are included in the range of $\pm 3\sigma$ of the results of MCS in short-period range. It can be said the conditions of MCS used in this study have the reproducibility of observed ground motions.

5. Discussion

The multiple linear regression analysis was conducted for examining the sensitivities of seismic-source characteristics to response spectra of synthetic ground motions. The pseudo velocity response of synthetic waves is set as objective variable (output), and seismic-source characteristics with uncertainties in Table 1 are set as explanatory variables (input). To equivalently evaluate the sensitivity of the input variables to the output variable, the multiple liner regression analysis was performed with normalized input and output variables whose means are 0, standard deviations are 1. It is assumed that the pseudo velocity responses of synthetic wave can be expressed as the linear combination of the seismic-source parameters x_i (i =1, 2, …, m) and residual ε, such as Eq. 11.

$$y(T) = a_0(T) + a_1(T)x_1 + a_2(T)x_2 + \cdots + a_m(T)x_m + \varepsilon \qquad (11)$$

where, $a_0(T)=0$, $a_i(T)$ (i=1,2, ..., m): regression coefficients. Fig. 7 shows regression coefficients of each seismic-source characteristic. The upper figure shows parameters related to asperity, such as size and location, and the lower figure

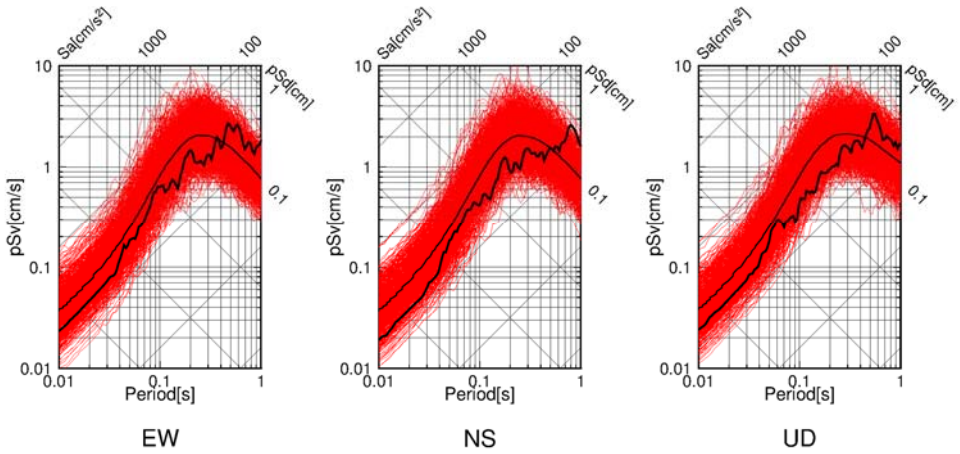

Figure 5. Response spectra (pSv, h=5%) of synthetic ground motions at KMMH01 (red lines). Black thick lines show observed records, and black thin lines show median of synthetic ground motions.

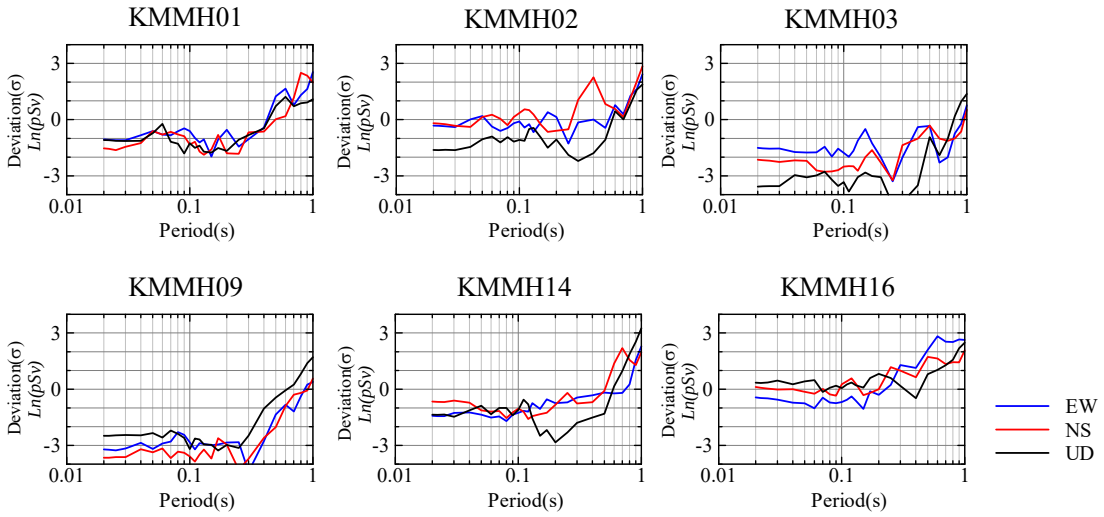

Figure 6. Deviations of the observed response spectra

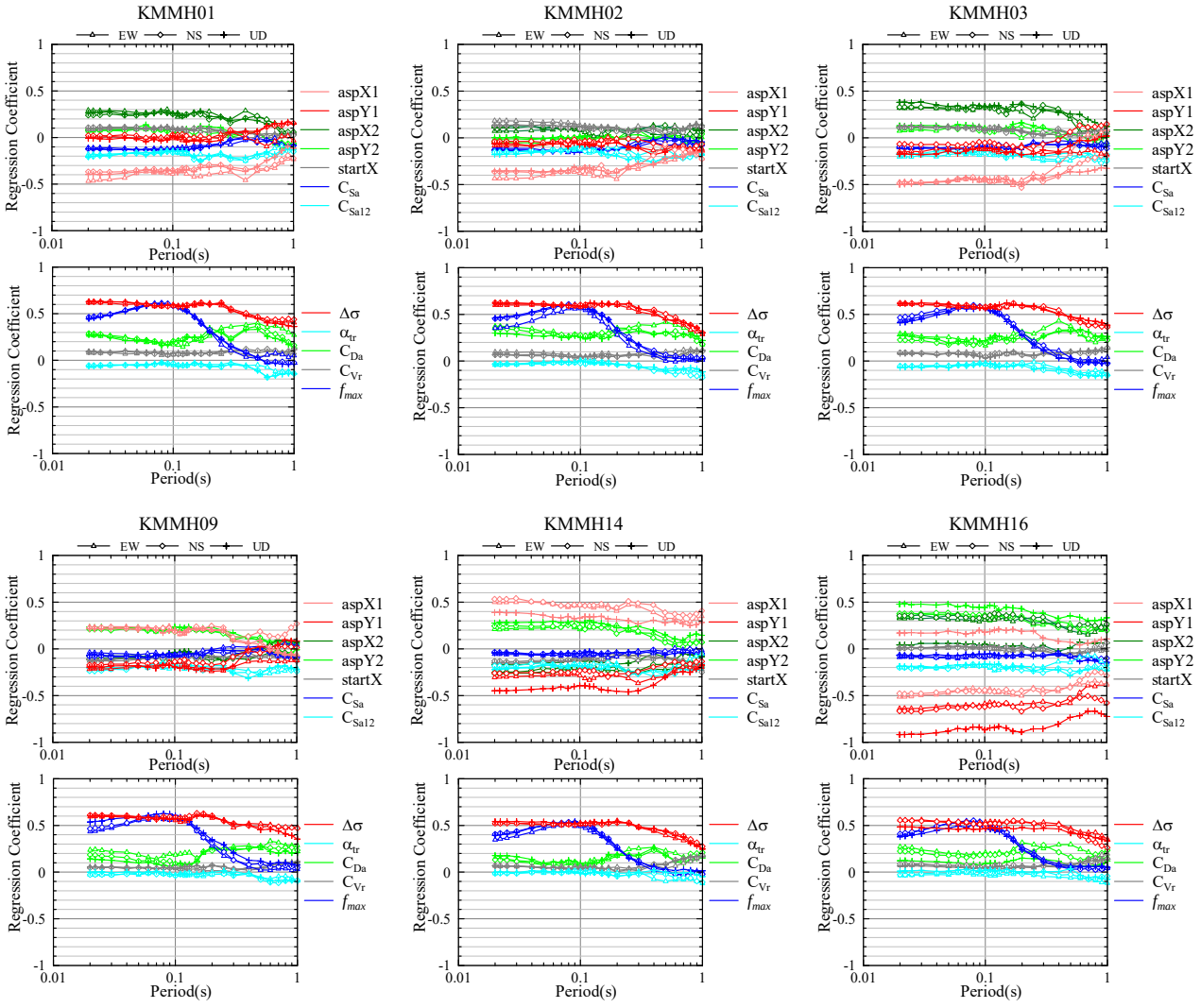

Figure 7. Regression coefficients spectra for each characteristic

shows other parameters. The sensitivity of $\Delta\sigma$,α_{tr}, C_{Da}, C_{Vr}, and f_{max} shows a similar trend between all stations. On the other hand, the sensitivity of the parameters related to location of asperities, such as *aspX1*, *aspY1*, *aspX2*, or *aspY2* depends strongly on the relative location of the station to fault asperity. The closer the location of asperity to a station, the stronger the response become, therefore the higher the sensitivity is obtained as for the parameters related to location of asperities.

As a result, it was found that seismic-source parameters $\Delta\sigma$, f_{max}, and location of 1st asperity show high sensitivity to pseudo velocity response. In case of the foreshock, the deviation of $\Delta\sigma$ is -0.79σ, f_{max} is 0.00ζ, *aspX1* is -0.16σ and *aspY1* is -1.39σ (shown in Table 2). The effects of the parameters which have the large absolute value of the deviation, $\Delta\sigma$ and *aspY1*, are discussed. $\Delta\sigma$, which has the negative deviation for the foreshock, has positive correlation to the MCS results, so it has the negative effect on the deviation of observed response spectra. As shown in Fig. 6, response spectra show negative deviations at KMMH01, KMMH02, KMMH03 and KMMH09. However, at KMMH14 and KMMH16, the deviations of observed records are larger than those at the other stations. This may be caused by the effect of *aspY1*. *aspY1* has negative correlations at KMMH14 and KMMH16, and has negative deviation for the foreshock. This means that *aspY1* has positive effect on the deviation of observed response spectra. This effect appears in Fig. 6. On the other hand, *aspY1* has low correlations to the MCS results at KMMH01, KMMH02, KMMH03, and KMMH09. (Fig. 7) It can be seen in Fig. 6 that observed response spectra have negative deviations at these stations.

6. Conclusion

Validation of the method to generate a lot of ground-motion time histories which incorporate seismic-source uncertainties by MCS was conducted. It was indicated that the simulated ground motions could cover observed ground motion level in short-period range. The multiple linear regression analysis yielded that $\Delta\sigma$, f_{max}, and location of 1st asperity had high sensitivity to pseudo velocity response of the MCS results.

In this study, however, only short-period range was targeted because SGFM could not reproduce the foreshock in long-period range. In a study by Igarashi et al. (2015), the hybrid method of SGMF and wave-number integration method were conducted to generate synthetic ground motions. It is necessary that we apply the hybrid method to generate synthetic ground motions.

References

Alfredo H.A., Wilson H.T. 2006. Probability Concepts in Engineering. *Wiley*

Asano K., Iwata T. 2016. Source rupture processes of foreshock and mainshock in the 2016 Kumamoto earthquake sequence estimated from the kinematic waveform inversion of strong motion data. *Earth Planet Sp*, 68, 147.

Headquarters for Earthquake Research Promotion 2016. Strong ground motion prediction method for earthquakes with specified source faults (“Recipe”)

Igarashi S., Sakamoto S., Nishida A., Muramatsu K., Takada T. 2015. Structural Response by Ground Motions from Sources with Stochastic Characteristics. *Proceedings of ICONE-23*. ICONE23-1548

Nishida A., Igarashi S., Sakamoto S., Uchiyama Y., Yamamoto Y., Muramatsu K., Takada T. 2015. Characteristics of Simulated Ground Motions Consistent with Seismic Hazard. *Nuclear Engineering and Design*, 295, 875-886.

Port and Airport Research Institute Web pages 2016. Characterized Source Model for 2016 Kumamoto earthquake (M6.5, Foreshock). (in Japanese) http://www.pari.go.jp/bsh/jbn-kzo/jbn-bsi/taisin/sourcemodel/somodel_2016kumamoto_z.html (accessed Jan. 15th 2020)

Uchiyama Y., Yamamoto Y. 2016. Short-period Spectral Level and Path Characteristics of the 2016 Kumamoto Earthquake Using Spectral Inversion Method. *Journal of JAEE*, 16, 10, 146-150

.